

Superconducting box coupled to a classical environment

Gert-Ludwig Ingold¹

Service de Physique de l'Etat Condensé, Commissariat à l'Energie Atomique, Saclay, F-91191 Gif-sur-Yvette Cedex, France

1. Introduction

The simplest system which exhibits Coulomb charging effects [1] is the so-called box circuit where a metallic island is coupled to a voltage source via a normal tunnel junction or a Josephson junction [2]. The number of electrons or Cooper pairs on a normal or superconducting island, respectively, is a good quantum number if the charging energy of the island is the dominant energy. As a consequence, the average number of electrons or Cooper pairs then shows clear steps as a function of the applied voltage. This so-called Coulomb staircase has been observed both in the normal [3] and in the superconducting case [4]. However, the charge quantization on the island will never be perfect. Finite temperatures lead to fluctuations of the island charge and thus to a rounding of the steps. Another source of fluctuations is in the superconducting case the finite Josephson coupling without which a change of the island charge would be impossible. Correspondingly, in the normal case a finite tunneling resistance leads to fluctuations of the island charge [5].

Since a few years it is known that mesoscopic systems often may not be considered as independent from their

surroundings. The behavior of a single ultrasmall tunnel junction, for example, depends strongly on the electromagnetic environment of the junction [6]. The influence of the environment on the superconducting box was studied recently [7] and it was found that even a low-frequency environment of sufficient strength may significantly reduce charge fluctuations on the island. This result was obtained by a mapping to the spin-boson problem for which the partition function could be determined from an exact summation of a perturbation series in the Josephson coupling.

The aim of the present paper is to give a more transparent discussion of the influence of a low-frequency impedance on the charge quantization on a superconducting island. In Section 2 we introduce the superconducting box which we couple to a classical environment in Section 3. Analytical results for the partition function within a two-state approximation are presented in Section 4. The average island charge may be calculated from the partition function. Results for zero and finite temperatures are given in Sections 5 and 6, respectively. Finally, in Section 7 we present our conclusions.

2. Superconducting box

The superconducting box circuit under consideration is shown in Fig. 1. An island is formed by a Josephson

¹ Present and permanent address: Lehrstuhl für Theoretische Physik I, Universität Augsburg, Memminger Str. 6, D-86135 Augsburg, Germany.

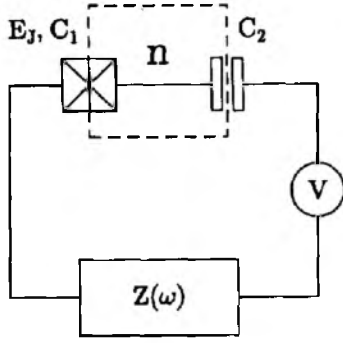


Fig. 1. Superconducting box circuit containing an island formed by a Josephson junction with Josephson coupling energy E_J and capacitance C_1 and a capacitor of capacitance C_2 . The island carrying n excess Cooper pairs is coupled to a voltage source via an impedance $Z(\omega)$.

junction and a capacitor. The junction is characterized by a Josephson coupling energy E_J and capacitance C_1 while the capacitor has a capacitance C_2 . Then $C_\Sigma = C_1 + C_2$ is the capacitance of the island leading to the charging energy $E_c = 2e^2/C_\Sigma$ for a single Cooper pair. The charge of the island is $-2ne$ where n is the number of excess Cooper pairs on the island. Here, we neglect the quasiparticles which is a good approximation if the gap energy Δ needed to create a quasiparticle on the island is much larger than the island charging energy E_c . The latter should always be larger than the thermal energy $k_B T$ in order to avoid a total suppression of charging effects by thermal fluctuations. One may shift the island charge by applying an external voltage V which results in an effective island charge $-2e(n - n_x)$ where $n_x = C_2 V / 2e$. [2] The Hamiltonian describing the charging energy of the island is therefore given by

$$H_c = E_c (n - n_x)^2. \quad (1)$$

The corresponding parabolas are shown in Fig. 2 together with the Coulomb staircase for the average number of excess Cooper pairs on the island. At zero temperature and for negligible Josephson coupling the staircase would be as ideal as shown.

The island capacitance C_Σ becomes more apparent in the circuit of Fig. 3 which may be obtained from the circuit of Fig. 1 by applying network transformation rules [6]. The transformed circuit also contains a modified environment consisting of the original impedance $Z(\omega)$ which now is in parallel with the total capacitance $C_{tot} = C_1 C_2 / (C_1 + C_2)$. The total capacitance is formed by the two capacitances of the Josephson junction and the capacitor in series shown in Fig. 1 as seen from the environment.

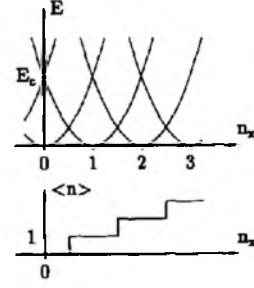


Fig. 2. Charging energy parabolas as a function of the external voltage $V = 2en_x/C_2$ according to Eq. (1). The different parabolas correspond to different island charges. Below the ideal Coulomb staircase for the average number of excess Cooper pairs on the island is shown.

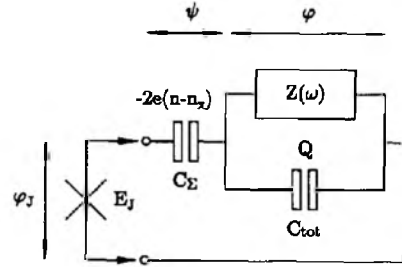


Fig. 3. Circuit equivalent to the box circuit shown in Fig. 1 if seen from the Josephson junction. $C_\Sigma = C_1 + C_2$ is the island capacitance while $C_{tot} = C_1 C_2 / (C_1 + C_2)$ is the capacitance of the two island capacitors as seen from the surrounding circuit. The phase differences across Josephson junction, island capacitor, and environment are indicated.

The tunneling of Cooper pairs through the Josephson junction is described by the Josephson Hamiltonian

$$H_T = -\frac{E_J}{2} \cos(\varphi_J), \quad (2)$$

where the phase difference φ_J across the junction is related to the voltage U across the junction by

$$\varphi_J = \frac{2e}{\hbar} \int^t dt' U(t'). \quad (3)$$

Correspondingly, we define phases φ for the environment and ψ for the island capacitance where U in Eq. (3) has to be replaced by the voltage across the environmental impedance and by $-2e(n - n_x)/C_\Sigma$, respectively. Since the voltages in the circuit of Fig. 3 add up to zero we may require that the phases add up to zero as well. Then φ_J may be replaced by $-\psi - \varphi$. We note that the phase

ψ and the excess number of Cooper pairs are conjugate variables obeying the commutation relation

$$[\psi, n] = -i. \quad (4)$$

Therefore, the operator $\exp(\pm i\psi)$ changes the island charge by $\mp 2e$. Correspondingly, the charge Q on the capacitor parallel to the environmental impedance shown in Fig. 3 and the phase φ are conjugate variables with the commutation relation

$$[\varphi, Q] = 2ie. \quad (5)$$

3. Classical environment

We now turn to the description of the environmental impedance of which we may think in terms of a set of harmonic oscillators. Starting with a Caldeira–Leggett-type Hamiltonian [8] it can be shown that any environmental impedance can be described by an appropriate choice of harmonic oscillators [6]. In the following, we restrict ourselves to a classical environment for which the frequencies of the oscillators are much smaller than the thermal frequency $k_B T/\hbar$. This type of environment may be treated adiabatically thus allowing for results which are nonperturbative in the Josephson coupling energy E_J . It is therefore especially suited for a theoretical study of environmental effects. In addition, experimentally one often has a low-frequency part of the environmental impedance which in principle may have arbitrary strength with a cutoff frequency in the MHz range, while the high-frequency impedance usually is very small and may be treated perturbatively. We note that the above condition for the environmental mode spectrum implies that zero temperature results are obtained by first taking the limit of zero frequency before taking the zero temperature limit. From an experimental point of view this is reasonable because frequencies in the MHz range and below correspond to temperatures of the order of 10^{-4} K and smaller which for most practical purposes can be considered as zero temperature.

For the calculation of the partition function oscillator modes with frequencies much below $k_B T/\hbar$ can effectively be considered as zero-frequency modes because the thermal time $\hbar\beta$ is too short to distinguish between a low but finite frequency and a zero-frequency mode. More formally, this can be shown by considering correlation functions [7]. We therefore may model the environment by one single mode with zero frequency leading to the environmental Hamiltonian

$$H_{\text{env}} = \frac{Q^2}{2C}. \quad (6)$$

We thus replace the total impedance $Z_t(\omega) = [i\omega C_{\text{tot}} + 1/Z(\omega)]^{-1}$ of Fig. 3 by a fictitious capacitor with capacitance C carrying the charge Q . The corresponding real part of the impedance is given by $(\pi/2C)\delta_+(\omega)$ where $\delta_+(\omega)$ is a delta function shifted infinitesimally to positive frequencies. Since this impedance has to contain the weight of all modes in the original total impedance, we relate the capacitance to the integrated real part of the impedance introduced in Ref. [7] by

$$a = \int_0^\infty d\omega \frac{\text{Re } Z_t(\omega)}{R_Q} = \frac{e^2}{\hbar C}, \quad (7)$$

where $R_Q = h/4e^2$ is the resistance quantum.

Collecting the Hamiltonians (1), (2), and (6) we obtain the total Hamiltonian

$$H = E_c(n - n_x)^2 + \frac{\hbar a}{2} \left(\frac{Q}{e}\right)^2 - \frac{E_J}{2} (e^{i(\psi - \varphi)} + e^{-i(\psi + \varphi)}). \quad (8)$$

The last term containing the phases φ and ψ conjugate to the environmental charge Q and the island charge $-2ne$, respectively, couples the tunneling to or from the island to the environment. The eigenenergies of Eq. (8) may be calculated with Q as a parameter after making the Hamiltonian independent of the environmental phase φ . In view of Eq. (4) we rewrite the operator $\exp(i\psi)$ in the charge representation as

$$e^{i\psi} = \sum_{n=-\infty}^{+\infty} |n-1\rangle\langle n|. \quad (9)$$

It then becomes clear that a unitary transformation which multiplies the charge state $|n\rangle$ by $\exp[i(n - \frac{1}{2})\varphi]$ will indeed lead to a φ -independent Hamiltonian. The shift of n by $\frac{1}{2}$ leads to a more symmetric formulation which will be convenient in Section 4. Making use of Eq. (5) we finally obtain the Hamiltonian

$$H = \sum_{n=-\infty}^{+\infty} \left[E_c \left[\left(n - \frac{1}{2}\right)^2 - \varepsilon(2n - 1) \right] + \frac{\hbar a}{2} \left(\frac{Q}{e} - 2n + 1\right)^2 \right] |n\rangle\langle n| - \frac{E_J}{2} \sum_{n=-\infty}^{+\infty} (|n\rangle\langle n+1| + |n+1\rangle\langle n|). \quad (10)$$

Here, we have introduced $\varepsilon = n_x - \frac{1}{2}$ which measures the distance from the step in the average island charge where the charge states $n = 0$ and 1 are degenerate. Furthermore, we have discarded the constant energy $E_c \varepsilon^2$ which is especially convenient when only two charge states are considered. From Eq. (10) we may directly calculate the partition function

$$\mathcal{Z} = \int_{-\infty}^{+\infty} dQ \text{Tr } e^{-\beta H}, \quad (11)$$

where the trace has to be taken over the island charge states. The average island charge may then be obtained according to

$$\langle n \rangle = \frac{1}{2} + \frac{1}{2\beta E_c} \frac{\partial \ln(\mathcal{Z})}{\partial \varepsilon} \quad (12)$$

from which the slope of the step is obtained as

$$\chi = \left. \frac{\partial \langle n \rangle}{\partial \varepsilon} \right|_{\varepsilon=0}. \quad (13)$$

In general, the partition function (11) has to be evaluated numerically. However, close to a step ($\varepsilon \ll 1$) it is often sufficient to restrict the calculation to two charge states. This case, for which analytical results may be derived, will be discussed in the following.

4. Partition function in two-state approximation

The steps in the average island charge appear at voltages for which two charge states are degenerate. At $\varepsilon = 0$ these are the states $n = 0$ and 1. We note that the behavior of the system is periodic in n so that all steps have the same form. Not too far from the step, i.e. for $\varepsilon \ll 1$, the restriction to these two charge states is still a good approximation provided that $E_J \ll E_c$. This ensures that the level splitting between the two states under consideration is much smaller than the energetic distance to the neglected states. In addition, we have to require $k_B T \ll E_c$ to avoid thermal excitation to other charge states and thermal suppression of charging effects. These conditions still allow for an arbitrary ratio $E_J/k_B T$.

Restricting the charge states in Eq. (10) to $n = 0$ and 1 we get for the Hamiltonian in matrix notation

$$H = \begin{pmatrix} E_c \varepsilon + \frac{\hbar a}{2} \left(\frac{Q}{e} + 1 \right)^2 & -\frac{E_J}{2} \\ -\frac{E_J}{2} & -E_c \varepsilon + \frac{\hbar a}{2} \left(\frac{Q}{e} - 1 \right)^2 \end{pmatrix}, \quad (14)$$

where we shifted the energy by $E_c/4$. The first and second component of the state vector are related to $|n\rangle = |0\rangle$ and $|1\rangle$, respectively. From Eq. (14) we immediately get for the eigenenergies as a function of the environmental charge Q

$$E_{1,2} = \frac{\hbar a}{2} \left(\frac{Q}{e} \right)^2 + \frac{\hbar a}{2} \pm \left[\left(\frac{E_J}{2} \right)^2 + \left(\hbar a \frac{Q}{e} + E_c \varepsilon \right)^2 \right]^{1/2}. \quad (15)$$

The behavior of the ground state energy as a function of Q changes qualitatively at $\hbar a = E_J/2$. For the case of

weak coupling ($\hbar a < E_J/2$) shown in Fig. 4 the ground state energy has only one minimum while for the case of strong coupling ($\hbar a > E_J/2$) shown in Fig. 5 the ground state energy displays two minima. In the two figures the left curve is given for a voltage at the step ($\varepsilon = 0$) while the right curve corresponds to a voltage in the vicinity of the step ($\varepsilon = E_J/E_c$). Such energy curves have been obtained before for the spin-boson problem [9].

In order to understand this qualitative difference between the weak and strong coupling we consider the situation at the step ($\varepsilon = 0$). The connection of the superconducting box to an electromagnetic environment leads to a coupling between the island charge and the environmental charge. For weak Josephson coupling this results in eigenstates of the Hamiltonian which are also good eigenstates of the number operator for Cooper pairs on the island. Since we consider only two charge states we get the corresponding two minima in the strong coupling case of Fig. 5. On the other hand, for weak coupling to

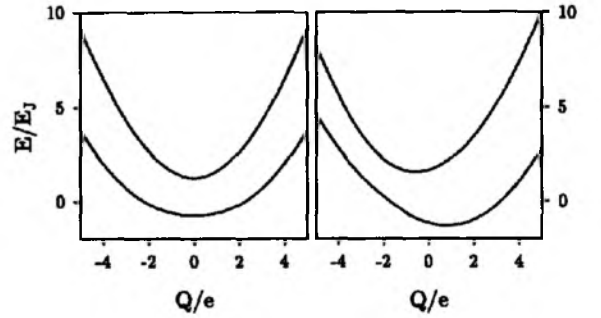


Fig. 4. The two energies (15) as a function of the environmental charge Q for weak coupling $\hbar a = 0.25E_J$. The left and right curves correspond to $\varepsilon = 0$ and E_J/E_c , respectively.

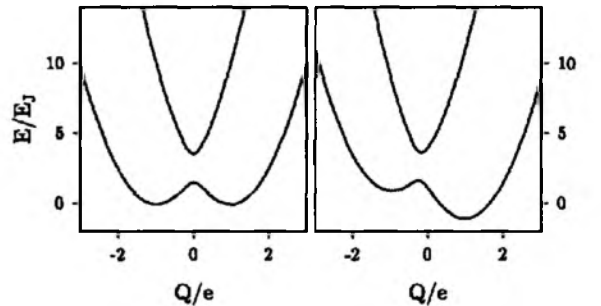


Fig. 5. The two energies (15) as a function of the environmental charge Q for strong coupling $\hbar a = 2.5E_J$. The left and right curves correspond to $\varepsilon = 0$ and E_J/E_c , respectively.

the environment the Josephson coupling energy is dominant. This leads to a strong hybridization of the two charge states. As a consequence the charge oscillator is frustrated which results in an energy minimum at $Q = 0$. It follows from this discussion that the different number of local minima will have direct consequences for the behavior of the superconducting box. This will become clear in Section 5 where we consider the case of zero temperature.

The partition function within the two-state approximation follows from Eq. (11) as

$$\mathcal{Z} = \int_{-\infty}^{+\infty} dQ [e^{-\beta E_1(Q)} + e^{-\beta E_2(Q)}], \quad (16)$$

which together with Eq. (15) becomes

$$\mathcal{Z} = \int_{-\infty}^{+\infty} dx \exp \left[-\beta \left(\frac{\hbar a}{2} x^2 + \frac{\hbar a}{2} \right) \right] \times \cosh \left[\beta \left(\left(\frac{E_J}{2} \right)^2 + (\hbar a x + E_c \varepsilon)^2 \right)^{1/2} \right]. \quad (17)$$

By expanding the integrand it can be shown that this result is equivalent to the somewhat more complicated expression for the partition function given in Eq. (50) of Ref. [7] apart from the partition function of the free environment which was divided out in the latter result. In general, the partition function (17) has to be evaluated numerically. Analytical results can be obtained for zero temperature as well as for low temperatures with $k_B T < E_J$ where a local harmonic approximation around the energy minima is possible. The expressions for the position of the minima as well as the corresponding harmonic approximations for the energy are given in the appendix.

5. Zero-temperature behavior

Results for zero temperature may be obtained by considering the minima of the charge-dependent ground state energy. As was already discussed in Section 3 this is no zero-temperature limit in the strict sense since according to our model the thermal energy always has to be larger than the mode energy of the oscillator. Nevertheless, the following results are valid for temperatures which for practical purposes can be considered as zero temperature.

In order to calculate the behavior of the average number of excess Cooper pairs on the island it is convenient to determine from Eq. (14) the charge state of the ground state from which the average charge as a function of the

environmental oscillator charge Q and the distance ε from the step is obtained as

$$\langle n \rangle(Q, \varepsilon) = \frac{\left(E_Q - \left[\left(\frac{E_J}{2} \right)^2 + E_Q^2 \right]^{1/2} \right)^2}{2 \left[\left(\frac{E_J}{2} \right)^2 + E_Q^2 - E_Q \left[\left(\frac{E_J}{2} \right)^2 + E_Q^2 \right]^{1/2} \right]} \quad (18)$$

with

$$E_Q = \hbar a \frac{Q}{e} + E_c \varepsilon. \quad (19)$$

Since for our two-state model $\langle n \rangle$ gives the probability to find the state $n = 1$, Eq. (18) confirms the arguments given above. For $\varepsilon = 0$ we find for large Josephson coupling energy a strong hybridization corresponding to $\langle n \rangle = \frac{1}{2}$. On the other hand, for small Josephson coupling energy we get $\langle n \rangle = 0$ or 1 depending on the sign of Q .

For weak coupling ($\hbar a < E_J/2$) the slope of the average number of excess Cooper pairs as a function of the applied voltage at $\varepsilon = 0$ is determined by the continuous shift of the minimum of the ground state energy as shown in Fig. 4. Inserting the leading ε -dependence of Q_0 given in Eq. (A.1) into Eq. (19) we obtain from Eq. (18) for the slope

$$\chi = \frac{E_c}{E_J - 2\hbar a}. \quad (20)$$

This result diverges as $\hbar a = E_J/2$ is approached which indicates that for stronger coupling $\langle n \rangle(\varepsilon)$ exhibits a jump.

For strong coupling ($\hbar a > E_J/2$) the behavior changes qualitatively because of the two minima which are present in the ground state energy shown in Fig. 5. For nonzero ε the energy curve is asymmetric and the lower minimum will determine the average number of excess Cooper pairs. At $\varepsilon = 0$ the two minima are degenerate leading to a finite jump of $\langle n \rangle$. According to Eq. (A.3) the degenerate environmental charges at the minima of the ground state energy are

$$\frac{Q_{\pm}}{e} = \pm \left[1 - \left(\frac{E_J}{2\hbar a} \right)^2 \right]^{1/2}. \quad (21)$$

Together with Eqs. (18) and (19) we then get for the jump of $\langle n \rangle$ at $\varepsilon = 0$

$$\Delta \langle n \rangle = \left[1 - \left(\frac{E_J}{2\hbar a} \right)^2 \right]^{1/2}. \quad (22)$$

As we expect, the height of the jump goes to zero as $\hbar a$ approaches $E_J/2$ from above.

6. Finite temperature results

We now consider the case of low but finite temperatures for which $E_J/k_B T \gg 1$. Then thermal fluctuations are rather small allowing us to study the interplay between Josephson coupling and environmental coupling. Furthermore, for the calculation it is sufficient to consider only the ground state energy and to expand the energy around the minima up to second order.

For weak coupling we make use of Eq. (A.2) to calculate the partition function. Together with Eqs. (12) and (13) we get for the slope of the step

$$\chi = \frac{E_c}{E_J - \hbar a} \left(1 - \frac{6\hbar a}{\beta(E_J - 2\hbar a)^2} \right), \quad (23)$$

which yields to first order in the coupling strength a ,

$$\chi = \frac{E_c}{E_J} \left[1 + \frac{2\hbar a}{E_J} \left(1 - \frac{3}{\beta E_J} \right) \right]. \quad (24)$$

Since we have $\beta E_J \gg 1$ these result describe an increase of the slope due to the coupling to the environment. If we include the excited state with Eq. (A.6) into the calculation of the partition function, we find to first order in a ,

$$\chi = \frac{E_c}{E_J} \tanh\left(\frac{\beta E_J}{2}\right) + \hbar a \left[3 \frac{E_c}{E_J^2} - \frac{6E_c}{\beta E_J^3} \tanh\left(\frac{\beta E_J}{2}\right) - \frac{E_c}{E_J^2} \tanh^2\left(\frac{\beta E_J}{2}\right) \right]. \quad (25)$$

This expression also contains the result for small Josephson coupling, $\beta E_J \ll 1$ given in Ref. [7].

For strong coupling we use Eq. (A.4) to obtain for the slope

$$\chi = \frac{\beta E_c}{2} \left[1 - \left(\frac{E_J}{2\hbar a} \right)^2 \right] + \frac{E_c}{2\hbar a} \frac{E_J^2}{((2\hbar a)^2 - E_J^2)}, \quad (26)$$

where we neglected terms of order T . For very strong coupling the slope takes the asymptotic value $\beta E_c/2$. The first term in Eq. (26) also describes the leading behavior in the opposite temperature limit $\beta E_J \ll 1$ for strong coupling $\hbar\beta a \gg 1$. [7].

The dependence of the slope on the coupling strength is shown in Fig. 6. The dashed line shows the zero-temperature result (20) which diverges at $\hbar a = E_J/2$ since the slope for stronger coupling is infinite. The full line has been calculated numerically from Eq. (17) for the finite temperature $k_B T = 0.02 E_J$. The corresponding analytical results (23) and (26) based on the harmonic approximation of the energy are shown as dotted lines. They are in

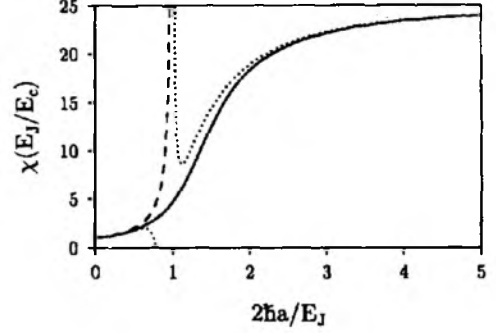


Fig. 6. Slope χ of $\langle n \rangle$ at a step as a function of the coupling strength $\hbar a$. The full line was calculated numerically for $\beta E_J = 50$. The corresponding analytical results obtained from the harmonic approximation of the energy are shown as dotted lines. The dashed line corresponds to zero temperature.

good agreement with the numerical curve except in the vicinity of $\hbar a = E_J/2$ where the character of the ground state energy changes. The figure shows that an environmental impedance may increase the slope significantly, especially at low temperatures.

7. Conclusions

We have studied a superconducting box circuit which contains a low-frequency environment of arbitrary strength. Within the approximation of two charge states it was found that the behavior of the system changes qualitatively when the integrated real part of the impedance exceeds the value $E_J/2\hbar$. The model of one zero-frequency mode relates this to the qualitative change in the dependence of the ground state energy on the environmental charge. At zero temperature strong coupling to the environment leads to a jump of the average island charge at the voltage where two charges are degenerate. At low but finite temperatures the slope at the step can be increased significantly by the environment thus leading to a better charge quantization.

Acknowledgement

The author would like to thank V. Bouchiat, M. H. Devoret, D. Estève, H. Grabert and F. Neumann for inspiring discussions. This work was carried out at the Centre d'Etudes de Saclay whose hospitality is gratefully acknowledged. Financial support was provided by the Deutsche Forschungsgemeinschaft through the Heisenberg program.

Appendix: Energy minima and harmonic approximation

For low temperatures it is useful to consider the vicinity of the energy minima in harmonic approximation. In the following we list the charges Q_0 for which the energy is minimal for small ϵ as well as the energies for small ϵ up to second order in the distance ΔQ from Q_0 . For the ground state the minimum charge in the case of weak coupling ($\hbar a < E_J/2$) is given by

$$\frac{Q_0}{e} = \frac{2E_c}{E_J - 2\hbar a} \epsilon - \frac{4E_c^3 E_J}{(E_J - 2\hbar a)^4} \epsilon^3 + \dots \quad (\text{A.1})$$

and the energy reads

$$E = -\frac{E_J}{2} + \frac{\hbar a}{2} - \frac{E_c^2}{E_J - 2\hbar a} \epsilon^2 + \left[\frac{\hbar a}{2} - \frac{(\hbar a)^2}{E_J} + 6 \frac{(\hbar a)^2 E_c^2}{E_J(E_J - 2\hbar a)^2} \epsilon^2 \right] \left(\frac{\Delta Q}{e} \right)^2 + \dots \quad (\text{A.2})$$

For strong coupling ($\hbar a > E_J/2$) the ground state energy has two minima at

$$\frac{Q_0}{e} = \pm \left[1 - \left(\frac{E_J}{2\hbar a} \right)^2 \right]^{1/2} + \frac{E_c E_J^2}{\hbar a} \frac{1}{(\hbar a)^2 - E_J^2} \epsilon \mp 12 \frac{E_c^2 E_J^2 \hbar a}{((2\hbar a)^2 - E_J^2)^{5/2}} \epsilon^2 + \dots \quad (\text{A.3})$$

Expanding the energy around these minima we obtain

$$E = -\frac{E_J^2}{8\hbar a} \mp E_c \left[1 - \left(\frac{E_J}{2\hbar a} \right)^2 \right]^{1/2} \epsilon - \frac{2E_c^2 E_J^2}{\hbar a} \frac{1}{(2\hbar a)^2 - E_J^2} \epsilon^2 + \left[\frac{\hbar a}{2} \left(1 - \left(\frac{E_J}{2\hbar a} \right)^2 \right) \pm \frac{3E_c E_J^2}{4\hbar a} \frac{1}{[(2\hbar a)^2 - E_J^2]^{1/2}} \right] \epsilon$$

$$+ \frac{3E_c^2 E_J^2}{2\hbar a} \frac{2(2\hbar a)^2 - E_J^2}{((2\hbar a)^2 - E_J^2)^2} \epsilon^2 \left] \left(\frac{\Delta Q}{e} \right)^2 + \dots \quad (\text{A.4})$$

Independent of the coupling strength the excited state has only one minimum at

$$\frac{Q_0}{e} = -\frac{2E_c}{E_J + 2\hbar a} \epsilon + \frac{4E_c^3 E_J}{(E_J + 2\hbar a)^4} \epsilon^3 + \dots \quad (\text{A.5})$$

The energy close to this minimum is given by

$$E = \frac{E_J}{2} + \frac{\hbar a}{2} + \frac{E_c^2}{E_J + 2\hbar a} \epsilon^2 + \left[\frac{\hbar a}{2} + \frac{(\hbar a)^2}{E_J} - 6 \frac{(\hbar a)^2 E_c^2}{E_J(E_J + 2\hbar a)^2} \epsilon^2 \right] \left(\frac{\Delta Q}{e} \right)^2 + \dots \quad (\text{A.6})$$

References

- [1] For a survey see: H. Grabert and M.H. Devoret (eds.), Single Charge Tunneling, Coulomb Blockade Phenomena in Nanostructures, NATO ASI Series B, Vol. 294 (Plenum Press, New York, 1991).
- [2] D. Esteve, in Ref. [1].
- [3] P. Lafarge, H. Pothier, E.R. Williams, D. Esteve, C. Urbina and M.H. Devoret, Z. Phys. B 85 (1991) 327.
- [4] P. Lafarge, P. Joyez, D. Esteve, C. Urbina and M.H. Devoret, Nature 365 (1993) 422.
- [5] See e.g., K.A. Matveev, Zh. Eksp. Teor. Fiz. 99 (1991) 1598 [Sov. Phys. JETP 72 (1991) 892]; H. Grabert, Physica B 194-196 (1994) 1011.
- [6] G.-L. Ingold and Yu. V. Nazarov, in Ref. [1].
- [7] F. Neumann, G.-L. Ingold and H. Grabert, Phys. Rev. B, to appear.
- [8] A.O. Caldeira and A.J. Leggett, Ann. Phys. (NY) 149 (1983) 374.
- [9] R. Graham and M. Höhnnerbach, Z. Phys. B 57 (1984) 233; B. Carmeli and D. Chandler, J. Chem. Phys. 82 (1985) 3400.